Soft Matter

ROYAL SOCIETY OF CHEMISTRY

COMMUNICATION

View Article Online
View Journal | View Issue

Cite this: *Soft Matter*, 2021, **17**, 7260

Received 15th June 2021,
Accepted 9th July 2021

DOI: 10.1039/d1sm00890k

rsc.li/soft-matter-journal

Linear triglycerol-based fluorosurfactants show high potential for droplet-microfluidics-based biochemical assays†

Mohammad Suman Chowdhury, [a] Wenshan Zheng,[b] Abhishek Kumar Singh,[a] Irvine Lian Hao Ong, [c] Yong Hou,[a] John A. Heyman, [d] Abbas Faghani,[a] Esther Amstad, [c] David A. Weitz [d] and Rainer Haag *[a]

Fluorosurfactants have expanded the landscape of high-value biochemical assays in microfluidic droplets, but little is known about how the spatial geometries and polarity of the head group contribute to the performance of fluorosurfactants. To decouple this, we design, synthesize, and characterize two linear and two dendritic glycerol- or tris-based surfactants with a common perfluoropolyether tail. To reveal the influence of spatial geometry, we choose inter-droplet cargo transport as a stringent test case. Using surfactants with linear di- and triglycerol, we show that the inter-droplet cargo transport is minimal compared with their dendritic counterparts. When we encapsulated a less-leaky sodium fluorescent dye into the droplets, quantitatively, we find that the mean fluorescence intensity of the PFPE-dTG stabilized PBS-only droplets after 72 h was ~3 times that of the signal detected in PBS-only droplets stabilized by PFPE-lTG. We also demonstrate that the post-functionalization of PFPE-lTG having a linear geometry and four hydroxy groups enables the 'from-Droplet' fishing of the biotin–streptavidin protein complex without the trade-off between fishing efficiency and droplet stability. Thus, our approach to design user-friendly surfactants reveals the aspects of spatial geometry and facile tunability of the polar head groups that have not been captured or exploited before.

Droplet microfluidics has gained a momentum in bioanalytics where millions of pico- to nanoliter-volume drops are created, monitored, and sorted at kHz rates.[1] These drops are often metastable, leading to premature coalescence, and to enhance their metastability fluorosurfactant is employed.[2] However, cell-mimetic micro- and nano-compartments have also been engineered for a variety of biological studies using phospholipids and polymer-based surfactants.[3] Typically, the fluorosurfactant is dissolved in a compatible bio-inert-fluorinated oil that contains a high amount of dissolved oxygen and is immiscible in aqueous and organic solvents, making it an ideal platform for immersing biomolecule captured droplets.[4,5] This feature has galvanized many exciting micro-droplets based research and product developments in chemistry and biology,[2] including synthesis of small organic molecules,[6] single-cell barcoding,[7] single-cell ChIP-seq,[5] directed enzymatic evolution,[8] therapeutic antibody discovery,[9] combinatorial drug screening,[10] and digital ELISA.[11] To produce the water-in-fluorinated oil (w/o) emulsion droplets, typically, poly(dimethyl siloxane) (PDMS)-based microfluidic devices are used which provide an unprecedented control over droplet size, droplet scalability, and droplet analyses, covering a broad spectrum of miniaturized applications requiring a high-throughput platform.[12]

Commercially available PEG-PFPE$_2$, poly(ethylene glycol)-perfluoropolyether tri-block fluorosurfactant, is widely used to make monodisperse emulsion droplets.[13] Although it enables many droplet-based applications, it primarily suffers from four key issues: rapid inter-droplet molecular transport, low droplet stability, synthesis complexity due to the use of polydisperse polymer chains, and batch-to-batch variation, limiting its use in high-throughput drug-screening and directed enzymatic evolution.[14–18] Ultimately, the droplets stabilized with this surfactant do not resemble a sealed micro-reactor that should not suffer from these limitations. To address these issues, we recently reported a dendronized di-block fluorosurfactant that clearly outperformed the PEG-PFPE$_2$ surfactant in many aspects.[15] Even though other small polar molecules, such as oligo(ethylene glycol), monosaccharides, and poly(ethylene glycol), have been used to generate di-block PFPE surfactants, they often suffer from droplet instability.[19,20] However, fluorosurfactant with hexaethylene glycol was found to be more

[a] *Institut für Chemie und Biochemie, Freie Universität Berlin, Takustrasse 3, 14195 Berlin, Germany. E-mail: haag@chemie.fu-berlin.de*
[b] *Department of Chemistry and Chemical Biology, Harvard University, Cambridge, Massachusetts 02138, USA*
[c] *Soft Materials Laboratory, Institute of Materials, École Polytechnique Fédérale de Lausanne, 1015 Lausanne, Switzerland*
[d] *School of Engineering and Applied Sciences, Department of Physics, Harvard University, 29 Oxford Street, Cambridge, MA 02138, USA*

† Electronic supplementary information (ESI) available. See DOI: 10.1039/d1sm00890k

effective than its cyclic crown ether counterpart.[19] Remarkably, an earlier study shows that, although both linear and dendritic small compounds can have the same molecular weight, their spatial geometries can profoundly influence the anti-fouling properties of a 2D surface modified with a self-assembled monolayer (SAM),[21] justifying the importance of different spatial geometries of small molecules in different respects.

Furthermore, fluorosurfactants that can be readily post-modified to customize the droplet interface are scarce. Although heterobifunctional PEG-based di-block copolymer fluorosurfactants have been reported, they are not user friendly either because of the tedious synthesis protocols of their effective head groups before surfactant synthesis, lack of controllable coupling reaction, and purification complexity as PEG-based surfactants readily form emulsion with organic solvents, or because they often compromise with the stability of the droplets, their monodispersity, and, most importantly, with the number of functional groups at the droplet interface.[22,23] Hence, a fluorosurfactant that can be readily post-modified with a wide variety of chemical functionalities, using a facile and user-friendly chemistry, and easily purified in a high yield is advantageous. Therefore, novel polar groups that can meet these requirements are needed to design and synthesize a tunable fluorosurfactant and to cover a broad spectrum of bioanalytics in microfluidic droplets.

Here, we contribute to the goal of rational surfactant design, demonstrate a new microfluidic device for parallel droplet generation, and report four surfactants containing either a linear or a dendritic spatial geometry with three and four hydroxy groups and a common fluoro-tail. Using thin layer chromatography, we measured their polarity indices to explore how different polarities can potentially alter their physicochemical functions. In addition, we evaluated their surface tension values to demonstrate whether a polar head group with different spatial geometries can alter the surface activity of the surfactants and influence downstream applications. When these surfactants were tested to stabilize micro-droplets and minimize inter-droplet small-molecule transfer, we detected that although they could stabilize the droplets, their performance in cargo retention varied significantly. This is particularly important because a high cargo retention capability can greatly increase the data quality of drug-screening assays. Besides, we chose PFPE-lTG, the best-performing surfactants among all, for post-modification. We found that it can be easily customized under mild conditions. Most importantly, the functional surfactant could generate robust water-in-oil emulsions and provide a reactive droplet interface which would allow the selective extraction of molecules of interest from the droplet interior to the droplet interface; we refer this as 'fishing biomolecules from droplet'. Moreover, the functional surfactant can be easily purified and could be isolated in a high yield. We thus systematically exploit the aspects of these surfactants with respect to inter-droplet molecular transport and from-droplet fishing. In addition, we provide some novel insights into the effective fluorosurfactant design. It was indeed a serendipity that we found the linear triglycerol to be the best performer despite having equal number of hydroxy groups to the dendritic triglycerol.

To synthesize linear and dendritic di-block fluorosurfactants, we freshly prepare activated perfluoropolyether (PFPE) tails, bearing acyl chloride at the terminal, which further react with acetal-protected, amine-containing head groups to generate a stable amide bond between the tail and the head groups. Following a facile acetal deprotection under mild acidic conditions, the head groups become highly polar which creates a di-block fluorosurfactant, typically, in high yields of 70–80%. We employed excess of the head group components to achieve full conversion of the activated fluorous tail. As fluorous solvents such as HFE7100 and HFE7500 are immiscible in organic solvents,[4] multiple post-reaction washings with an excess of either methanol or dimethylformamide (DMF) removes the unreacted head groups and other possible impurities. We synthesize two triglycerol-based surfactants, both having four hydroxy (–OH) groups and a commercial PFPE tail: one is a linear triglycerol, lTG, and the other is a dendritic triglycerol, dTG. The surfactants produce a linear and a dendritic diblock surfactants: PFPE-lTG and PFPE-dTG, respectively (Fig. 1). In addition, we also synthesized two surfactants that were composed of three OH groups containing linear diglycerol or tris and a PFPE tail, creating PFPE-lDG or PFPE-Tris, respectively (Fig. 1).

Both the less polar PFPE-lDG and PFPE-Tris surfactants help us demonstrate three crucial things: how the interfacial tension (IFT) may vary due to the lack of one –OH, the minimum number of –OH groups needed to obtain an optimal droplet stability and cross-check the impact of three-hydroxy-carrying linear or dendritic spatial geometries with the four-hydroxy-carrying linear or dendritic one, respectively. Although different spectroscopic methods can be used to characterize the surfactants, for instance, NMR and IR,[22] we analyzed them using thin layer chromatography on silica plates (TLC) to investigate the polarity index of all four surfactants by means of a retardation factor (R_f), which would otherwise be extremely difficult using the available spectroscopic means due to solubility issues. We found that PFPE-dTG and PFPE-lTG showed marginally different R_f values: $\sim$0.33 and $\sim$0.3, respectively despite having an equal number of hydroxy groups. By contrast, PFPE-Tris had a maximum R_f of $\sim$0.46 among all four surfactants, whereas its counterpart PFPE-lDG had R_f $\sim$0.41 (see Fig. 2a and Fig. S2, ESI†). We attribute this polarity variation between the surfactants containing equal hydroxy groups to the ratio of primary *vs.* secondary hydroxy groups in the head groups, reflecting their different interactions with the polar silica surface. Additionally, we found no unreacted PFPE-COOH in the surfactant bands, qualitatively, suggesting that no PFPE acid impurity was left and the amide coupling between the polar head and the non-polar tail was successful.

To understand the influence of the –OH group number and spatial geometry of the head on interfacial tension (IFT), we tested the surface tension of all four surfactants. We use 1% surfactant by weight in HFE7500 oil to measure the IFT in MQ water. We found that PFPE-dTG reduces the IFT more than the other three surfactants do, where IFTs of PFPE-lTG and PFPE-Tris show significantly higher values, indicating different

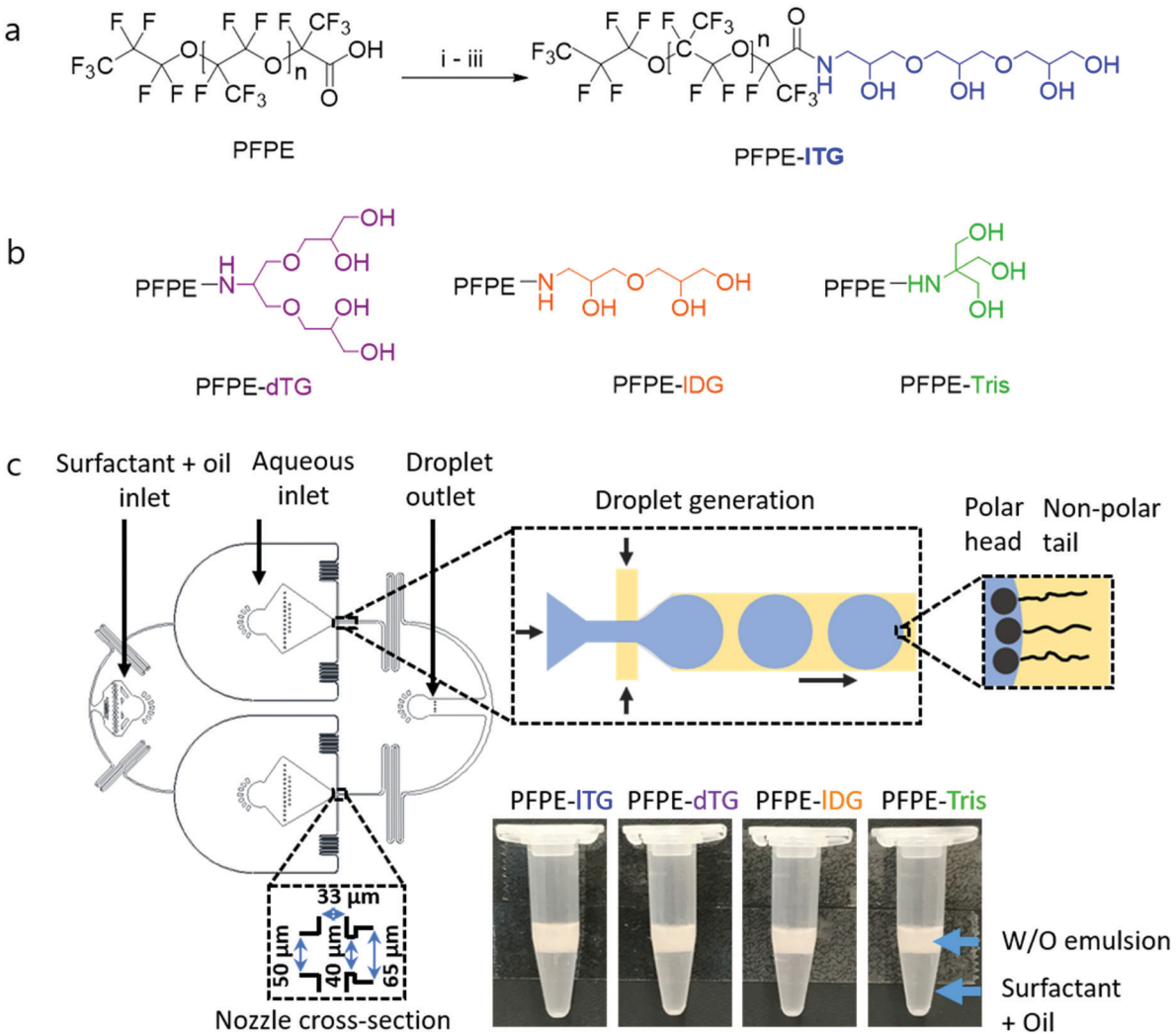

Fig. 1 (a) Synthetic approach to linear triglycerol fluorosurfactant through amide coupling: (i) $(COCl)_2$, HFE7100, cat. DMF, rt, overnight; (ii) acetal protected linear triglycerol-NH_2, TEA, rt, overnight; and (iii) H^+, CH_3OH-HFE7100, reflux, overnight. (b) Schematic illustration of the surfactants with different head groups. (c) A microfluidic approach for parallel droplet generation (left). Top insets show the droplet pinch-off at the nozzle area and the orientation of the perfluoropolyether-based surfactant molecules at the interface of water (light blue) and oil (yellow). The polar head groups are shown using black circles and the non-polar tail groups are shown using black wavy lines. Dimension of the nozzle cross-section is shown on the bottom left inset. The height of the channel was 50 µm. The 15 mm long serpentines after the nozzles were used to allow the surfactant molecules to better adsorb at the water–oil interface. A further detail of a microfluidic setup and a parallel droplet making PDMS chip are shown in Fig. S1, ESI†. The bottom right panel shows the droplet emulsions generated using surfactants with four different polar head groups. Emulsions were collected in Eppendorf tubes where the white layer contains the emulsion droplets, and the residual surfactant solution (transparent) remains below the emulsion layer because of the high density of HFE7500 oil (ρ = 1.614 g mL^{-1}).

surface interactions (Fig. 2b). However, the different IFT profiles of the fluorosurfactants did not cause a similar variation in the case of droplet size distribution (see Fig. S3, ESI†), while we generated the droplets at the constant oil and aqueous flow rates for all fluorosurfactants. For each surfactant, the droplet size distribution analysis demonstrated that the mean average droplet diameter remained within the range of ~90–93 µm, which suggests that the variation in droplet diameter is primarily governed by the geometry of the microfluidics channel and by the flow rates of oil and water.

Although the difference in the IFT values between PFPE-lTG and PFPE-dTG surfactants is at the minute level, this result encouraged us to investigate the inter-droplet molecular transport behavior by these surfactants to justify a known concept that a higher IFT is advantageous to reduce the inter-droplet molecular transport.[24] Besides, this stringent test helps to understand how the linear or dendritic spatial geometry of the four-hydroxy-containing surfactants PFPE-lTG or PFPE-dTG, respectively, influence the inter-droplet molecular transport.

To test the inter-droplet molecular transport, we used 3 µM sodium fluorescein salt as a water-soluble and less-leaky dye. By using a parallel droplet maker,[15] we produced a mixture comprising an equal proportion of PBS-only and PBS + fluorescein dye droplets. We collected the water-in-oil emulsion droplets in an Eppendorf tube and incubated them at 37 °C.

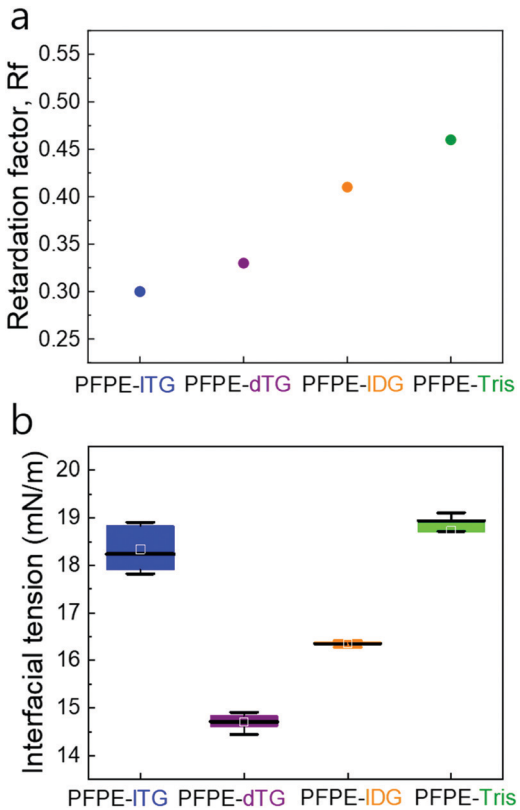

Fig. 2 (a) R_f values on silica indicating the polarity of fluorosurfactants (left). A mixture of 20% methanol (v/v) and HFE-7100 was used as the elution solvent. (b) Interfacial tension (IFT) of the fluorosurfactants measured under identical test conditions (right) by the hanging drop method. Deionized water and 1% (w/w) surfactant containing HFE-7500 oil were used to measure the IFT between the water drop and HFE-7500 oil at 25 °C. To obtain the average IFT value five measurements were performed.

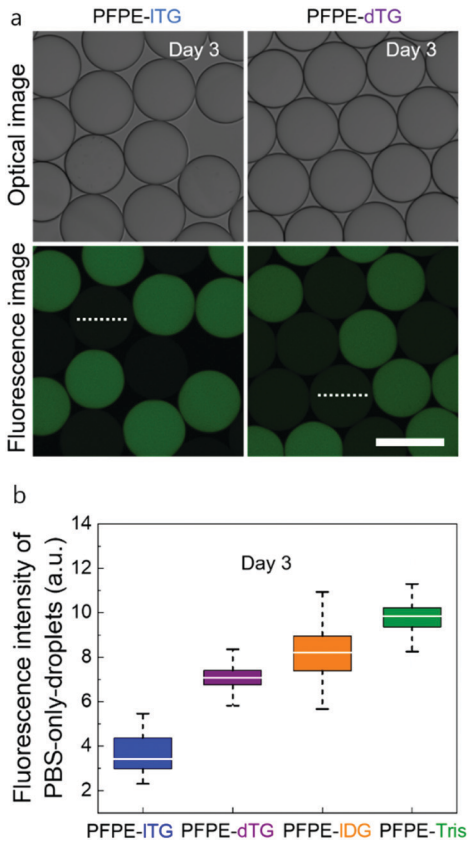

Fig. 3 (a) Micrographs showing the inter-droplet diffusion of a fluorescence dye sodium fluorescein salt after 72 h where two populations of empty and dye-containing droplets were stabilized with PFPE-lTG or PFPE-dTG. Two representative initially empty droplets are marked using dotted lines characteristic for intensity measurements. (b) A quantitative fluorescence intensity analysis of five randomly selected PBS-only-droplets using Image J plot profiling tool where the droplets were stabilized with either PFPE-lTG, PFPE-dTG, PFPE-lDG, or PFPE-Tris after three days (see Fig. S4, ESI†). Scale bar, 100 μm.

Surprisingly, droplets stabilized with the linear PFPE-lTG surfactant were found to prevent inter-droplet dye diffusion more than those that had been stabilized with its dendritic counterpart, PFPE-dTG (Fig. 3a). Quantitatively, on day 3, the mean green fluorescence signal of PFPE-dTG stabilized PBS-only drops was ~3 times the signal detected in PBS-only drops stabilized by PFPE-lTG, which suggested that, although both the surfactants were featuring four –OH groups, both the spatial geometry and the slightly different surface tension were playing pivotal roles in displaying different transport behaviors (Fig. 3a and b). Additionally, we assume that the marginal polarity variation due to different spatial geometries and ratios of primary *vs.* secondary –OH groups in the polar heads could also impact the cargo retention phenomena. Furthermore, when we tested the three –OH group containing surfactants, we found that the linear diglycerol-based surfactant, PFPE-lDG, performed slightly better than its dendritic counterpart PFPE-Tris (as shown by the difference between the mean intensity values in Fig. 3b), even though there is no big difference in their surface tension values measured, justifying the undeniable influence of head group polarity. Clearly, these data suggest that a higher surface tension alone is not the deciding factor to control the inter-droplet leaching, rather the number of –OH groups, ratio of primary *vs.* secondary –OH groups, the overall polarity, and the head group's spatial geometry, collectively, play a major role in controlling the inter-droplet transport kinetics. The study of inter-droplet transport kinetics with the 3 μM sodium fluorescein salt also revealed that for each fluorosurfactant a minimal leakage at day 1 and day 2 occurs when compared to the leakage on day 3 (see Fig. S5, ESI†). To gain more insights, we further investigated the inter-droplet transport behavior using 10 μM sodium fluorescein salt where we used only the triglycerol-based fluorosurfactants. Under this test condition, a quantitative analysis showed that both the fluorosurfactants showed a significant amount of dye leakage on day 3. However, PFPE-lTG performed marginally better than PFPE-dTG (see Fig. S6, ESI†), which suggests that the higher the concentration of the dye, the higher will be the inter-droplet leakage. To demonstrate that the superior performance of PFPE-lTG is not dye selective, we then tested both the triglycerol-based fluorosurfactants using 2 μM resorufin sodium salt. This fluorescence dye is more-leaky and shows inter-droplet leakage at a time scale of minutes.[15] Under this testing condition, after 30 min of incubation, the intensity profile of the

PBS-only-droplets stabilized with PFPE-lTG showed a repeating trend of minimal leakage compared to the droplets stabilized with PFPE-dTG. This justified that the minimal inter-droplet leakage offered by PFPE-lTG is independent of the dye types (see Fig. S7, ESI†). Overall, we think a linear polar head group with a minimum of four hydroxy groups is needed to design a more effective surfactant when leakage of small molecule is concerned. We further investigated the ability of the linear and dendritic surfactants to stabilize ~95 micron-sized large droplets prior to and during PCR reactions at an elevated temperature. Surprisingly, we found that during the miniaturized PCR reactions, surfactant with dendritic-triglycerol effectively stabilized the droplets with no merging, but when the linear-triglycerol-based surfactant was used nearly 50% droplets merged and the remaining 50% droplets were polydisperse (Fig. S8, ESI†). By contrast, the emulsion droplets merged completely when they were stabilized with the linear or dendritic surfactants lacking hydroxy groups, justifying two crucial things: irrespective of the spatial geometry a minimum of four hydroxy groups is inevitable and a dendritic spatial geometry is the key to stabilize the droplets during high temperature reaction. The high performance of PFPE-lTG to achieve a minimal inter-droplet leakage and its spatial geometry motivated us to exploit it further by post-functionalization for more sophisticated applications such as from-droplet fishing of a protein complex. It is worth mentioning that a PEG-based di-block copolymer fluorosurfactant can also be used for post-modification, but since it cannot make robust and monodisperse droplets, for quantitative analysis, it is unattractive to use the PEG-based di-block copolymer surfactants.[20,22] We, therefore, investigated the post-modification of the linear triglycerol surfactant with bromoacetic acid followed by substitution of the bromine with azide (Fig. 4a). The covalently coupled azido moiety in the linear triglycerol head can be clearly confirmed by the strong azide signal at ~2100 cm^{-1} in FT-IR spectroscopy (Fig. 4b). Besides, the FT-IR data also confirmed a newly formed ester bond by displaying the ester signal ~1750 cm^{-1}. Moreover, when the functional surfactant reacted with slightly excess of cyclooctyne containing DBCO-PEG4-Biotin, the azide peak ~2100 cm^{-1} disappeared, and the ester peak remained, confirming that the click reaction was successful. Although azido acetic acid is commercially available, we wanted to demonstrate that a multi-step post-modification could be easily conducted which is not feasible with the widely used commercial PEG-based tri-block copolymer surfactant PEG-$PFPE_2$, because there is no reactive site in its main chain.

We used a single-drop maker-device to generate ~70 micron-sized droplets with the azide-coupled linear surfactant PFPE-lTG-N_3 (Fig. 5a). We employed one equivalent of bromo acetic acid to react with statistically one –OH per head group, incorporating one azide functionality per surfactant molecule. Using PFPE-lTG-N_3, we first encapsulated strained cyclooctyne-containing DBCO-Sulfo-Cy-3 fluorophore in the aqueous core of the droplet. We found that under this tested condition this functional surfactant effectively fishes from 5 to 10 μM DBCO-Sulfo-Cy-3 within 10 minutes *via* the azide–cyclooctyne click reaction (Fig. S9, ESI†). Next, we tested a more complex system that consisted of biotin and streptavidin. It is worth mentioning that the protein complex of biotin and streptavidin is widely used in many biosensing applications, in which streptavidin carries four biotin binding sites, offering multivalency for many applications, including robust cross-linking,[25] antibody–drug conjugation,[26] capturing antibody, and antigen.[27] However, the biotin–streptavidin interaction is highly sensitive to its surroundings, such as linker chemistry, ionic concentration, pH, and hydrogen-bonding, making the assay highly tricky unless the reaction conditions are optimized.[28,29] Therefore, we used Milli-Q water and freshly prepared the protein complex using one equivalent of Cy5-streptavidin (M_W ~ 60 000 g mol^{-1}) and eight equivalents of DBCO-PEG4-Biotin, providing two biotins for each

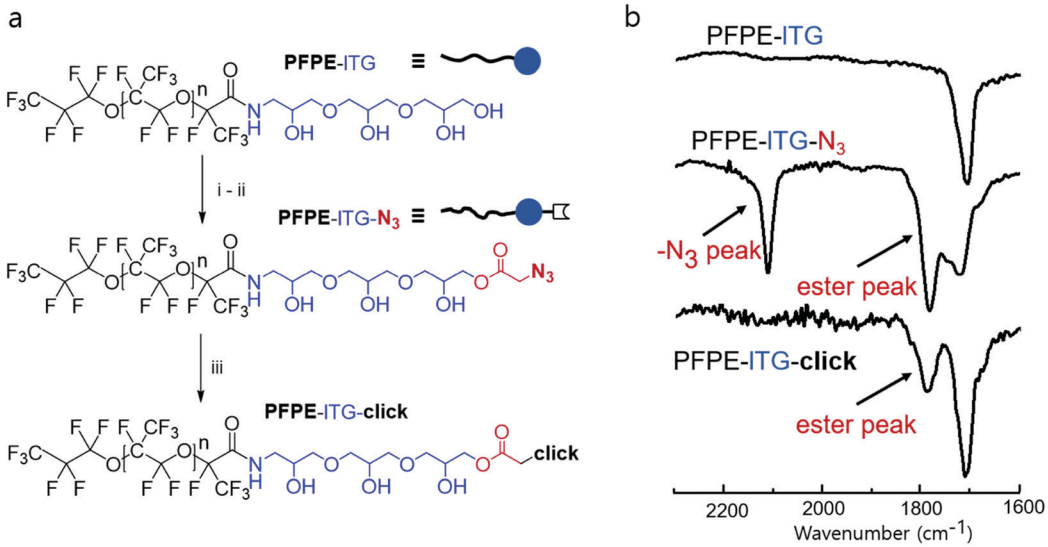

Fig. 4 (a) Post-modification of PFPE-lTG by esterification: (i) bromoacetic acid, EDC·HCl, DMAP, DMF-HFE7500; (ii) NaN_3, DMF-HFE7500; and (iii) DBCO-PEG4-Biotin, CH_3OH-HFE7100. (b) FT-IR spectra showing the presence of azide and ester in the modified PFPE-lTG-N_3 surfactant, absence of both in the pristine surfactant, and disappearance of the azide signal after the click reaction.

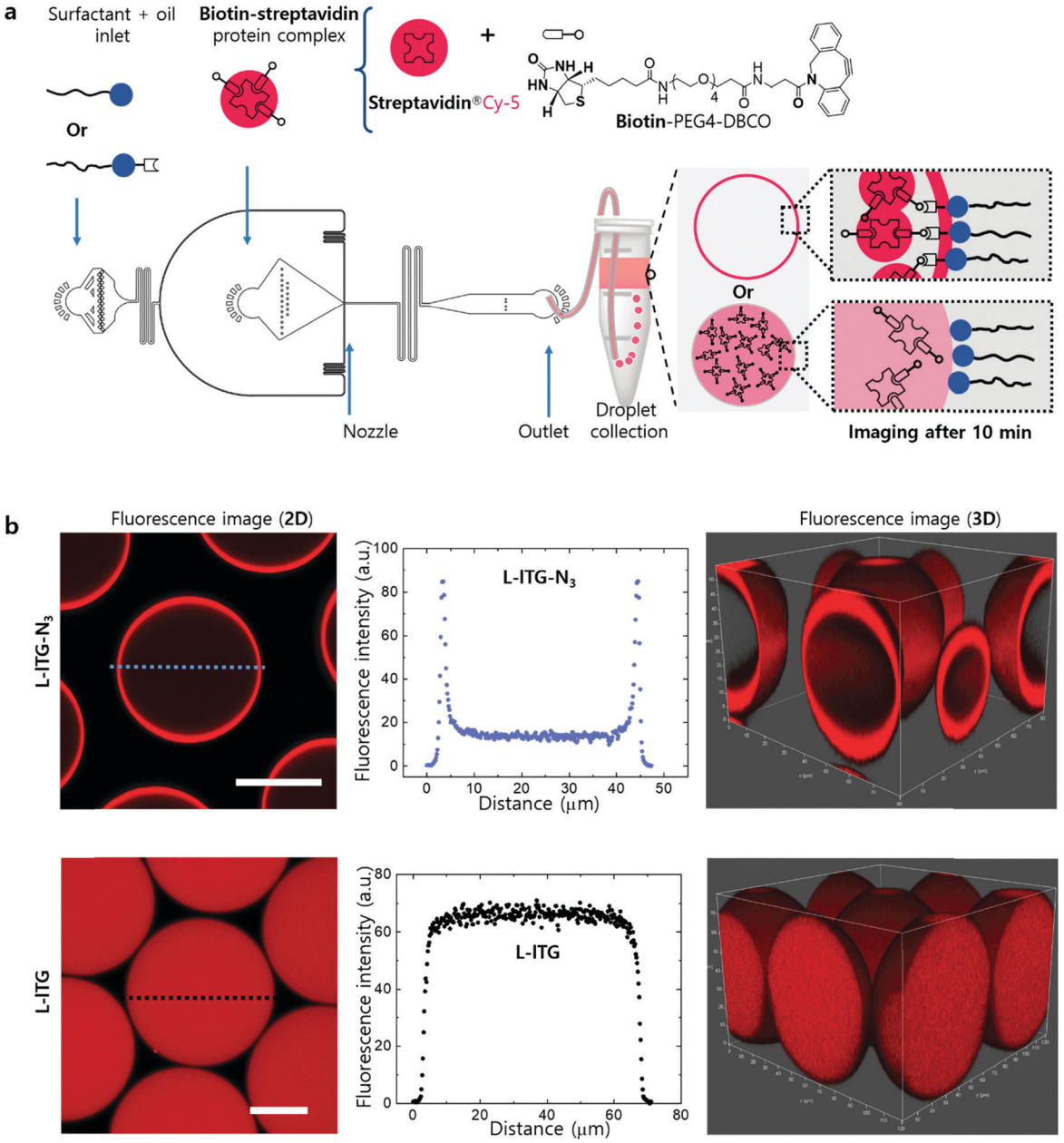

Fig. 5 (a) Schematics of a PDMS-based single droplet maker-device to encapsulate biotin–streptavidin protein complex mixture in microdroplets, and a water-in-oil emulsion droplet stabilized with either PFPE-lTG-N_3 or PFPE-lTG surfactant, illustrating the from-droplet fishing ability by each surfactant individually. The single droplet making device had the same nozzle cross-section as mentioned earlier for the parallel droplet making device in Fig. 1c. Here, the protein complex is comprised of DBCO-PEG4-Biotin and streptavidin®Cy-5. (b) 2D and 3D confocal fluorescence images of the protein complex encapsulated droplets stabilized with either PFPE-lTG-N_3 (top row) or PFPE-lTG (bottom row) surfactant. Unlike PFPE-lTG, PFPE-lTG-N_3 enables the from-droplet fishing *via* azide–cyclooctyne click reaction between surfactant and protein complex, which is clearly shown by the strong fluorescence intensity at the droplet interface. Images were taken 10 minutes after droplet generation. Scale bars, 25 μm.

biotin-binding site in the streptavidin. In this way, we found that using the PFPE-lTG-N_3 surfactant, from-droplet fishing of the biotin–streptavidin protein complex could also be conducted effectively within 5–10 minutes after encapsulation (Fig. 5b). Undoubtedly, the from-droplet biomolecules fishing approach can be highly useful for droplet-based bioanalytical assay, requiring capture and immobilization of target molecules at the droplet interface, that would benefit from this readily tunable functional surfactant in many aspects. For example, droplet-based rapid isolation of therapeutic cells can be conducted[30] where the surfactants can be functionalized with a capture antibody before or after droplet generation. Thus, it will eliminate the need of beads decorated with capture antibody and ultimately simplify the droplet-based cell-isolation assay.

In summary, relative to dendritic triglycerol, and those lacking hydroxy groups, triglycerol with a linear spatial geometry appears to be the most effective polar head group for a minimal inter-droplet leakage of a water-soluble fluorescein dye.

Consequently, we envision that linear triglycerol-based fluorosurfactants have high potential as robust and easily sourced water-in-oil emulsion stabilizers. Most importantly, they are extremely useful to improve the data quality of assays such as droplet-based high-throughput drug screening which should not suffer from inter-droplet leakage.

Additionally, we show that a multi-step post-modification of the linear triglycerol-based surfactant can be easily performed to alter its chemical functionality by grafting a small functional group to the hydroxy group. Thus, when an azido moiety was linked to the linear triglycerol head, the post-functionalized surfactants effectively stabilized the droplets, created a reactive droplet interface, and enabled from-droplet fishing, in addition to providing biocompatibility. Which hints, to alter the chemical environment of the droplet interface, other biomolecules or small molecules with diverse functional groups could also be easily coupled to the linear triglycerol-based fluorosurfactants without trading off the stability of the droplets and their monodispersity. Additionally, the on-demand tunability of the fluorosurfactants can be further explored, for example, to discover therapeutic antibodies by screening single B cells where the functional surfactants will be the alternatives to the bead-based assays. This new linear triglycerol-based fluorosurfactant offers a broad range of user-defined biochemical assays in microfluidic droplets.

Author contributions

Mohammad Suman Chowdhury (M. S. C.) designed the research, synthesized the surfactants, analyzed the data and wrote the manuscript. Wenshan Zheng (W. Z.) designed the research, performed the PCR studies and analyzed the data. Abhishek Kumar Singh (A. K. S.) and M. S. C. jointly synthesized the head groups. Irvine Lian Hao Ong (I. L. H. O.) performed the interfacial tension measurements. Yong Hou (Y. H.) and M. S. C. jointly worked on the confocal imaging and analysis of the confocal data. John Heyman (J. H.) analyzed the data. Abbas Faghani (A. F.) and M. S. C. jointly purified the surfactants and analyzed the data. Esther Amstad (E. A.) and David A. Weitz (D. A. W.) supervised the study. Rainer Haag (R. H.) supervised the study, analyzed the data and wrote the manuscript.

Conflicts of interest

Freie Universität Berlin and Harvard University have filed a patent on some of the surfactants. M. S. C., D. A. W., and R. H. are affiliated with these institutions and are co-inventors in the patent.

Acknowledgements

This work was funded by the Deutsche Forschungsgemeinschaft (DFG, German Research Foundation) – project id 387284271 – SFB 1349 Fluorine-Specific Interactions. This work was supported by the core-facility Biosupramol (www.biosupramol.de). M. S. C. thanks Dr Pradip Dey, Dr Raju Bej, and Dr Prabhusrinivas Yavvari for valuable discussions.

References

1 E. K. Bowman and H. S. Alper, *Trends Biotechnol.*, 2020, **38**, 701.
2 A. B. Theberge, F. Courtois, Y. Schaerli, M. Fischlechner, C. Abell, F. Hollfelder and W. T. S. Huck, *Angew. Chem., Int. Ed.*, 2010, **49**, 5846.
3 T. Trantidou, M. Friddin, Y. Elani, N. J. Brooks, R. V. Law, J. M. Seddon and O. Ces, *ACS Nano*, 2017, **11**, 6549.
4 I. Lim, A. Vian, H. L. van de Wouw, R. A. Day, C. Gomez, Y. Liu, A. L. Rheingold, O. Campàs and E. M. Sletten, *J. Am. Chem. Soc.*, 2020, **142**, 16072.
5 A. Rotem, O. Ram, N. Shoresh, R. A. Sperling, A. Goren, D. A. Weitz and B. E. Bernstein, *Nat. Biotechnol.*, 2015, **33**, 1165.
6 S. Mashaghi, A. Abbaspourrad, D. A. Weitz and A. M. van Oijen, *Trends Anal. Chem.*, 2016, **82**, 118.
7 A. M. Klein, L. Mazutis, I. Akartuna, N. Tallapragada, A. Veres, V. Li, L. Peshkin, D. A. Weitz and M. W. Kirschner, *Cell*, 2015, **161**, 1187.
8 B. Kintses, C. Hein, M. F. Mohamed, M. Fischlechner, F. Courtois, C. Lainé and F. Hollfelder, *Chem. Biol.*, 2012, **19**, 1001.
9 K. Eyer, R. C. L. Doineau, C. E. Castrillon, L. Briseño-Rao, V. Menrath, G. Mottet, P. England, A. Godina, E. Brient-Litzler, C. Nizak, A. Jensen, A. D. Griffiths, J. Bibette, P. Bruhns and J. Baudry, *Nat. Biotechnol.*, 2017, **35**, 977.
10 A. Kulesa, J. Kehe, J. E. Hurtado, P. Tawde and P. C. Blainey, *Proc. Natl. Acad. Sci. U. S. A.*, 2018, **115**, 6685.
11 L. Cohen, N. Cui, Y. Cai, P. M. Garden, X. Li, D. A. Weitz and D. R. Walt, *ACS Nano*, 2020, **14**, 9491.
12 T. S. Kaminski, O. Scheler and P. Garstecki, *Lab Chip*, 2016, **16**, 2168.
13 L. Mazutis, J. Gilbert, W. L. Ung, D. A. Weitz, A. D. Griffiths and J. A. Heyman, *Nat. Protoc.*, 2013, **8**, 870.
14 P. Gruner, B. Riechers, B. Semin, J. Lim, A. Johnston, K. Short and J.-C. Baret, *Nat. Commun.*, 2016, **7**, 10392.
15 M. S. Chowdhury, W. Zheng, S. Kumari, J. Heyman, X. Zhang, P. Dey, D. A. Weitz and R. Haag, *Nat. Commun.*, 2019, **10**, 4546.
16 N. Shembekar, C. Chaipan, R. Utharala and C. A. Merten, *Lab Chip*, 2016, **16**, 1314.
17 O. Wagner, J. Thiele, M. Weinhart, L. Mazutis, D. A. Weitz, W. T. S. Huck and R. Haag, *Lab Chip*, 2016, **16**, 65.
18 Y.-L. Chiu, H. F. Chan, K. K. L. Phua, Y. Zhang, S. Juul, B. R. Knudsen, Y.-P. Ho and K. W. Leong, *ACS Nano*, 2014, **8**, 3913.
19 D. J. Holt, R. J. Payne, W. Y. Chow and C. Abell, *J. Colloid Interface Sci.*, 2010, **350**, 205.
20 C. Holtze, A. C. Rowat, J. J. Agresti, J. B. Hutchison, F. E. Angilè, C. H. J. Schmitz, S. Köster, H. Duan, K. J. Humphry, R. A. Scanga, J. S. Johnson, D. Pisignano and D. A. Weitz, *Lab Chip*, 2008, **8**, 1632.
21 M. Wyszogrodzka and R. Haag, *Langmuir*, 2009, **25**, 5703.
22 I. Platzman, J.-W. Janiesch and J. P. Spatz, *J. Am. Chem. Soc.*, 2013, **135**, 3339.

23 S. Ursuegui, M. Mosser and A. Wagner, *RSC Adv.*, 2016, **6**, 94942.
24 G. Etienne, A. Vian, M. Biočanin, B. Deplancke and E. Amstad, *Lab Chip*, 2018, **18**, 3903.
25 Y. Hu, A. S. Mao, R. M. Desai, H. Wang, D. A. Weitz and D. J. Mooney, *Lab Chip*, 2017, **17**, 2481.
26 D. Xu, A. J. Heck, S. L. Kuan, T. Weil and S. V. Wegner, *Chem. Commun.*, 2020, **56**, 9858.
27 A. S. Cheung, D. K. Y. Zhang, S. T. Koshy and D. J. Mooney, *Nat. Biotechnol.*, 2018, **36**, 160.
28 L. Cohen and D. R. Walt, *Bioconjugate Chem.*, 2018, **29**, 3452.
29 G. O. Reznik, S. Vajda, T. Sano and C. R. Cantor, *Proc. Natl. Acad. Sci. U. S. A.*, 1998, **95**, 13525.
30 R. Ding, K.-C. Hung, A. Mitra, L. W. Ung, D. Lightwood, R. Tu, D. Starkie, L. Cai, L. Mazutis, S. Chong, D. A. Weitz and J. A. Heyman, *RSC Adv.*, 2020, **10**, 27006.